Channeling in Sulfate Activating Complexes†

Meihao Sun and Thomas S. Leyh*

The Department of Biochemistry, Albert Einstein College of Medicine, 1300 Morris Park Avenue, Bronx, New York 10461-1926

Received March 2, 2006; Revised Manuscript Received June 8, 2006

ABSTRACT: The synthesis of activated sulfate (adenosine 5′-phosphosulfate, APS) and inorganic pyrophosphate from ATP and SO_4 is remarkably unfavorable: $K_{eq} \sim 10^{-8}$ under presumed, near-physiological conditions. Consequently, ATP sulfurylases, which catalyze APS synthesis, suffer $\sim 10^8$-fold losses in catalytic efficiency in the forward (APS-synthesis) versus reverse reaction. Losses of this magnitude place this catalyst at risk of being unable to supply its nutrients to the cell in a timely fashion. ATP sulfurylase domains are often embedded in multifunctional complexes that are capable of also catalyzing the second of two steps in the sulfate activation pathway: the phosphorylation of APS to produce PAPS (3′-phosphoadenosine 5′-phosphosulfate). The colocalization of these activities in a single scaffold suggests that evolution might have worked around the inefficiency problem by fashioning a system capable of transferring APS directly between the active sites of the complex, thereby avoiding the solution-phase energetics. For these reasons, representatives from each of the three types of sulfate activating complex (SAC) [*Homo sapiens* (type I); *Mycobacterium tuberculosis* (type II); and *Rhodobacter sphaeroides* (type III)] were tested for the ability to channel APS. A channeling assay that optically detects solution-phase APS was devised with APS reductase from *M. tuberculosis*, a previously uncharacterized enzyme. Channeling was not detected in two of the three types of SAC; however, the type III SAC channels with high efficiency. Structural models of type III reveal a 75 Å-long channel that interconnects active-site pairs in the complex and that opens and closes in response to occupancy of those sites.

Channeling, a process in which reactants pass between active sites without escaping into bulk solvent, offers a malleable dimension of protein function that can be used in a variety of ways for the evolutionary design of metabolism. Channeling requires molecular organization, which, by reducing entropy, can provide a driving force for biological function. Remarkable molecular architectures [tubes (*1*, *2*), grooves (*3*), and "swinging" arms (*4*)] that enable proteins to transfer reactants between catalytic sites have been described. Given a somewhat broader view of channeling (facilitated transfer of mass between two points in the cell), the phenomenon again comes into focus at higher levels of cellular organization: nuclear transport (*5*), molecular scaffolds (*6*), and kinesins (*7*). Beyond the general and intriguing issues associated with the relationships among entropy reduction, chemical work, and cellular function, channeling can be used in very specific ways to accomplish catalysis, and it is in these ways that it can assist the cell in the difficult catalytic task of activating sulfate.

The metabolic assimilation of sulfate, essential to life as we know it, requires that this stable, nonreactive compound be chemically activated. Once inside the cell, activation is accomplished by the enzyme ATP sulfurylase (ATP:sulfate adenylyltransferase, EC 2.7.7.4), which transfers the adenylyl moiety (AMP∼) of ATP from pyrophosphate to sulfate to form APS (adenosine 5′-phosphosulfate) (reaction 1). The Gibbs potential of the phosphoric/sulfuric acid anhydride bond (the chemical hallmark of activated sulfate) is quite large, $\Delta G'_{0\ \mathrm{hydrolysis}} \sim -19$ kcal/mol, and considerably greater than that associated with the hydrolysis of the α,β-bond of ATP, $\Delta G'_{0\ \mathrm{hydrolysis}} \sim -10.4$ kcal/mol (*8*−*10*). Consequently, the equilibrium constant for the forward, APS-forming reaction is extremely unfavorable; K_{eq} is estimated at $\sim 10^{-8}$ under presumed physiological conditions. To overcome this formidable energetic impediment, nature has embedded in certain ATP sulfurylases a GTPase domain whose turnover is stoichiometrically linked (1:1) to APS synthesis (reaction 2) (*11*, *12*). The second of two steps in the sulfate activation pathway is catalyzed by APS kinase, which phosphorylates APS at the 3′-hydroxyl of the ribose ring to produce PAPS (reaction 3), the sole sulfuryl group ($\sim SO_3^-$) donor in metabolism. Sulfuryl-transfer is used widely by the cell to regulate metabolism (*8*). In many organisms, the adenylyltransferase and APS kinase domains are found in a complex and, in certain cases, on a single polypeptide. These sulfate activating complexes (SACs) are the subject of this report.

$$ATP^{4-} + SO_4^{2-} \leftrightarrows + APS^{2-} + P_2O_7^{4-} \quad (1)$$

$$GTP^{4-} + H_2O \leftrightarrows GDP^{3-} + HPO_4^{2-} + H^+ \quad (2)$$

$$ATP^{4-} + APS^{2-} \leftrightarrows ADP^{3-} + PAPS^{4-} + H^+ \quad (3)$$

An enzyme's forward and reverse catalytic efficiencies are related by the Haldane equation: $(k_{cat}/K_m)_{for}/(k_{cat}/K_m)_{rev} =$

† Supported by the National Institutes of Health Grant GM54469.

* Corresponding author: phone 718-430-2857; fax 718-430-8565; e-mail leyh@aecom.yu.edu.

[1] Abbreviations. APS, adenosine 5′-phosphosulfate; EDTA, ethylenediaminetetraacetic acid; EST, estrogen sulfotransferase; Hepes, *N*-(2-hydroxyethyl)piperazine-*N*′-2-ethanesulfonic acid; PAPS, 3′-phosphoadenosine 5′-phosphosulfate; PNP, purine nucleoside phosphorylase; SA, specific activity (microcuries per milliliter); SAC, sulfate activating complex; unit, 1 micromole of product formed per minute at saturating substrate; TLC, thin-layer chromatography.

10.1021/bi060421e CCC: $33.50
Published on Web 09/02/2006

Table 1: Cloning Primers

enzyme	primer	sequence[a]
type I SAC	sense	***AATCATATG***GAGATCCCC
type I SAC	antisense	GAGCTCGAGAGCTTTCTC
type III SAC	sense	***GGAATTCCATATG***TCCCTTCCGAACCACGCTCCTGTCCCTGAAC
type III SAC	antisense	CGGGATCCGTCAGGCCCGGATCAGGCCCATCTGCTCGAGC
APS reductase	sense	***GGAATTCCATATG***AGCGGCGAGACAACCAGGCTGACC
APS reductase	antisense	CCGCTCGAGCTCCTCAGCATCGCTGCGCTCTGCATC
thioredoxin	sense	***GGAATTCCATATG***AGCGATAAAATTATTCACCTGACTGACGACAGTTTTG
thioredoxin	antisense	CCGCTCGAGCGGTTACGCCAGGTTAGCGTCGAGGAACTCTTTC

[a] Bold-italicized and underlined sequences are the *Nde*I and *Xho*I cleavage-site cassettes, respectively.

K_{eq} (*13*). This relationship requires that ATP sulfurylase be approximately 8 orders of magnitude less efficient in the forward direction. Enzymes achieve maximum catalytic efficiency when k_{cat}/K_m is equal to the rate constant governing diffusion of substrate to the active site (*14*), $\sim 10^8$ M^{-1} s^{-1}, and efficiencies are typically 1−3 orders of magnitude below this limiting value. Given these facts, the catalytic efficiency of ATP sulfurylase in the forward direction can be no greater than ~ 1 M^{-1} s^{-1}—a value so low that it puts the catalyst at risk of being unable to meet the nutrient demands of the cell. Thus, for those catalysts required to satisfy the cell's temporal nutrient constraints, the reaction equilibrium point can create a kinetic/efficiency barrier whose diminution requires solutions beyond the simple removal of product. Channeling provides such a solution because, in this case, the product, APS, does not enter solution, hence the overall, solution-phase equilibria do not apply—the surface of the enzyme becomes the "solvent." A second catalytic impediment that can be circumvented by channeling is the potent substrate inhibition by APS, which is common among APS kinase domains; APS binds most tightly to the active site in nonreactive modes, $K_i < 1$ μM (*10*, *15*−*17*). For these reasons, a representative from each of the three SAC classes was tested for its ability to channel APS.

MATERIALS AND METHODS

Lactate dehydrogenase (LDH) from rabbit muscle, glucose-6-phosphate dehydrogenase from yeast, pyruvate kinase (PK) from rabbit muscle, hexokinase from yeast, inorganic pyrophosphatase (PP_iase) from yeast, phenylmethylsulfonyl fluoride (PMSF), and pepstatin were purchased from Roche Applied Science. DNA restriction enzymes were acquired from New England Biolabs. Pfu Turbo polymerase was purchased from Stratagene. Chelating Sepharose and glutathione−Sepharose resins were obtained from Amersham. APS was synthesized and purified as described previously (*18*). Recombinant *Escherichia coli* ATP sulfurylase (*19*, *20*), yeast APS kinase (*18*), human estrogen sulfotransferase (*21*), and the sulfate activating complex from *Mycobacterium tuberculosis* (*10*) were expressed and purified as described previously. Recombinant HAL2 nucleotidase from yeast was expressed in BL21(DE3) cells and purified as described previously (*22*). PCR purification kits were obtained from Qiagen. $[^{35}S]SO_4^{-2}$ was purchased from MP Biochemicals, Inc. PEI-F TLC sheets were purchased from EM Science. Competent cells BL21(DE3) and BL21(DE3)pLysS were purchased from Novagen. PAPS was purchased from Professor S. Singer (University of Dayton, Dayton, OH). $MgCl_2$, ATP, ADP, AMP, PP_i, GTP, β-NADH, NAD^+, phosphoenolpyruvate (PEP), glucose, KOH, Na_2SO_4, EDTA, lysozyme, adenylate kinase (chicken muscle), β-mercaptoethanol (β-ME), reduced glutathione (GSH), *p*-nitrophenyl sulfate (*p*NPS), and dithiothreitol (DTT) were the highest grade available from Sigma. Glycerol, KCl, and Hepes were acquired from Fisher Scientific. Isopropyl 1-thio-β-D-galactopyranoside (IPTG) was purchased from Labscientific. Genomic DNA [*E. coli* (ATCC number 10798D), *Rhodobacter sphaeroides* (ATCC number 17023D) and human I.M.A.G.E. Consortium Clone (ATCC number 402569)] was obtained from ATCC. *M. tuberculosis* genomic DNA (H37Rv) was a generous gift from Dr. John Chan, from the Albert Einstein College of Medicine.

Cloning of Type I and III SAC, APS Reductase, and Thioredoxin. The cDNAs of the type I SAC (*Homo sapiens*, isoform I), type III SAC (*R. sphaeroides*), APS reductase (*M. tuberculosis*), and thioredoxin (*E. coli*) were PCR-amplified by use of the primers listed in Table 1. PCR products were purified by use of a PCR purification kit, cut with *Nde*I and *Xho*I, and subcloned into a dual-tag vector derived from the pGEX vector (*23*).

Protein Expression and Purification. The type I, II, and III SACs and APS reductase were expressed in BL21(DE3)-pLysS; thioredoxin was expressed in BL21(DE3). Cells harboring expression plasmid were grown at 37 °C to an OD_{600} of $\sim$0.7, the cultures were cooled to 16 °C, and inductant, IPTG, was then added to 0.80 mM. Following a 16 h incubation at 16 °C, the cells were pelleted, resuspended, and lysed by sonication, and debris was removed by centrifugation (*24*). The supernatant was loaded onto a chelating Sepharose column, which was then washed with buffer [K_2HPO_4 (50 mM, pH 7.3), KCl (0.40 M), β-ME (5.0 mM), and imidazole (10 mM)] and eluted with wash buffer containing imidazole (250 mM). Proteins were then loaded onto a second affinity resin, glutathione−Sepharose, nonspecific adsorbents were removed with wash buffer, and the fusion protein was eluted with buffer containing GSH (10 mM) and Tris-HCl (100 mM, pH 8.0). The affinity tags were proteolytically clipped from the fusion protein by use of Precission protease during overnight dialysis against Hepes/K^+ (25 mM, pH 7.5), KCl (50 mM), and DTT (2.0 mM) at 4 °C. The tags and protease were removed by passing the proteolysate through a glutathione−Sepharose column. The resulting proteins have five additional amino acids (GPLHM) attached to their N-termini. The purified enzymes, judged $\geq$95% pure by SDS−PAGE, were stored in dialysis buffer containing 5% glycerol at −70 °C. The calculated 280 nm extinction coefficients (ExPASy Proteomics Server) used to calculate protein active-site concentrations are as follows:

type I SAC (90.7 mM^{-1} cm^{-1}), type II SAC (76.8 mM^{-1} cm^{-1}), type III SAC (54.6 mM^{-1} cm^{-1}), APS reductase (36.1 mM^{-1} cm^{-1}), and *E. coli* thioredoxin (13.9 mM^{-1} cm^{-1}).

APS and PAPS as Substrates for APS Reductase. APS reductases typically utilize APS far more efficiently than PAPS; however, there appear to be exceptions that can reduce either substrate well (*25*). To determine the preference of the mycobacterial enzyme, its catalytic efficiency (k_{cat}/K_m) was determined with APS or PAPS as the substrate.

The reduction of APS was measured by coupling the AMP formed in the reductase-catalyzed reaction to the formation of 2 equiv of ADP [by use of adenylate kinase (*26*, *27*)], which were converted to ATP and, ultimately, to the oxidation of NADH (monitored by fluorescence, λ_{ex} 339 nm, λ_{em} 466 nm) via the PK/LDH coupling system (*28*). The mycobacterial APS reductase does not contain the C-terminal thioredoxin (*29*, *30*) domain present in other members of the family, and it therefore is expected to require thioredoxin or an alternative source of reducing equivalents. Titrations, not shown, established that APS reductase turnover is maximized in the channeling-assay buffer at the following reductant concentrations: thioredoxin (37 μM), glutathione (5.0 mM), and DTT (2.0 mM). The assay conditions used to determine V_m and $K_{m\ APS}$ were as follows: APS reductase (0.21 μM), PK (8.4 units/mL), LDH (18.0 units/mL), adenylate kinase (10 units/mL), thioredoxin (37.3 μM), $MgCl_2$ (3.0 mM), DTT (2.0 mM), ATP (1.0 mM), PEP (1.0 mM), EDTA (1.0 mM), GSH (5.0 mM), NADH (30 μM), and Hepes (50 mM, pH/K^+ 8.0), $T = 25 \pm 2$ °C. Reaction progress curves (from which constants were extracted) were initiated by adding 2.7 μM APS; SO_3^{2-} had no detectable effect on the progress curve at concentrations as high as 0.10 mM. The apparent constants obtained from this study are $K_{m\ APS} = 0.57$ ($\pm$0.01) μM and $k_{cat} = 9.2$ ($\pm$0.1) min^{-1}.

The reduction of PAPS was followed by optically monitoring transfer of the sulfuryl group of *p*-nitrophenyl sulfate (*p*NPS) to PAP (formed in the APS reductase reaction) by use of estrogen sulfotransferase (EST) (*31*, *32*). The *p*NPS to *p*-nitrophenol (*p*NP) conversion results in a change in absorbance at 400 nm. To set conditions for the APS reductase studies properly, the initial-rate parameters for the forward EST reaction with *p*NPS and PAP were determined under conditions similar to those used in the channeling experiments. The apparent K_m ($K_{m\ app}$) for PAP, 1.5 ($\pm$0.13) μM, was determined by holding *p*NPS at a fixed, saturating condition (10 mM, 18$K_{m\ app}$) and varying PAP concentration (0.24, 0.36, 0.72, 1.5, 3.0, 6.0, and 12 μM). Similarly, $K_{m\ app}$ for *p*NPS, 0.55 ($\pm$0.09) mM, was determined by varying *p*NPS concentration at a fixed, saturating concentration of PAP (1.0 mM, 700$K_{m\ app}$). Other reagents and conditions were identical: EST (4.0 μM), $MgCl_2$ (4.0 mM), DTT (2.0 mM), and Hepes (50 mM, pH/K^+ 8.0), $T = 25 \pm 2$ °C. Optical density was converted to concentration by use of an extinction coefficient of 16.9 mM^{-1} cm^{-1} (pH 8.0), which was determined from *p*NP standards. $k_{cat\ app}$ was 0.49 ($\pm$0.03) min^{-1}.

APS reductases typically utilize APS far more efficiently than PAPS; however, there appear to be exceptions that can reduce either well (*25*). To determine the substrate preference of the mycobacterial enzyme, and the catalytic efficiency (k_{cat}/K_m) toward APS, k_{cat} and K_m were determined with APS or PAPS as substrates under the following conditions: APS reductase (0.9 μM), PAPS (5.7, 11, 23, 34, 45, 57, 68, and 79 μM), EST (0.10 unit/mL), thioredoxin (37 μM), $MgCl_2$ (3.0 mM), DTT (2.0 mM), *p*NPS (10 mM), GSH (5.0 mM), and Hepes (50 mM, pH/K^+ 8.0), $T = 25 \pm 2$ °C. The apparent constants obtained from this study are $K_{m\ PAPS} = 31$ ($\pm$3.0) μM and $k_{cat} = 0.7$ ($\pm$0.3) min^{-1}.

In conclusion, the kinetic constants obtained for APS or PAPS [$K_{m\ APS} = 0.57$ ($\pm$0.01) μM, $k_{cat} = 9.2$ ($\pm$0.1) min^{-1}; $K_{m\ PAPS} = 31$ ($\pm$3.0) μM, $k_{cat} = 0.7$ ($\pm$0.3) min^{-1}] reveal that the enzyme reduces APS far more efficiently than PAPS: $(k_{cat}/K_m)_{APS}/(k_{cat}/K_m)_{PAPS} = 800$.

Initial-Rate Assays for the ATP Sulfurylase and APS Kinase Domains: (A) Type I SAC. The steady-state activity of the ATP sulfurylase domain was monitored by coupling APS formation to the production of ADP, by use of APS kinase, and ultimately to the oxidation of NADH by use of the PK/LDH coupling system (*28*). APS kinase, from yeast, was added to increase V/K_{APS}. Kinetic constants were obtained by determining initial rates as a function of the concentration of one substrate at a fixed, saturating concentration of the second. The conditions, which mimic those used in the channeling assays, are as follows: type I SAC (4.0 μM), SO_4^{2-} [fixed at 20 mM (41$K_{m\ app}$) or varied: 0.10, 0.20, 0.40, 0.60, 0.80, 1.2, 1.6, 2.0, 2.4, and 2.8 mM], ATP [fixed at 3.0 mM (58$K_{m\ app}$) or varied: 27, 54, 110, 16, 220, 270, and 320 μM], thioredoxin (37 μM), PK (8.0 units/mL), LDH (6.0 units/mL), PP_iase (1.0 unit/mL), APS kinase (6.0 units/mL), KCl (50 mM), DTT (2.0 mM), EDTA (1.0 mM), GSH (5.0 mM), PEP (3.0 mM), NADH (0.25 mM), $MgCl_2$ (5.0 mM), and Hepes (50 mM, pH 8.0), $T = 25 \pm 2$ °C.

Because the steady-state affinity of APS for APS kinase was quite high, $K_{m\ app}$ was determined by use of ^{35}S-APS, prepared as described previously (*33*). The assay conditions were as follows: type I SAC (2.5 nM), APS (3.0, 6.0, 13, 25, 50, 100, 250, or 500 nM), ATP [2.0 mM, 20K_m (*34*−*36*)], $MgCl_2$ (3.0 mM), PP_iase (0.5 unit/mL), KCl (100 mM), DTT (1.0 mM), and Hepes (50 mM, pH/K^+ 8.0), $T = 25 \pm 2$ °C.

(B) Type III SAC. The ATP sulfurylase assays were identical to those described for the type I system, with the following exceptions: type III SAC (0.2 μM), SO_4^{2-} [fixed at 20 mM (20$K_{m\ app}$) or varied: 0.5, 1.0, 2.0, 3.0, 8.0, and 13.0 mM], ATP [fixed at 3.0 mM (20$K_{m\ app}$) or varied: 14, 41, 97, 210, 430, and 870 μM].

The APS kinase reaction was followed by coupling the production of ADP to the oxidation of NADH, monitored at 339 nm, via the coupling enzymes PK and LDH. Initial rates were determined at each of the 16 conditions defined by a 4 × 4 matrix of APS and ATP concentrations. The assay conditions were as follows: type III SAC (25 nM), PK (8.0 units/mL), LDH (18 units/mL), HAL2 nucleotidase (0.5 unit/mL), APS (40, 59, 110, and 1000 nM), ATP (5.4, 7.9, 15, and 140 μM), PEP (1.0 mM), NADH (0.25 mM), $MgCl_2$ (2.0 mM), DTT (2.0 mM) and Hepes (50 mM, pH/K^+ = 8.0), $T = 25 \pm 2$ °C.

Homology Modeling of Type III SAC. Homology models of type III SAC were created with SWISS-MODEL (*37*, *38*) by use of the R- and T-state structures (*39*, *40*) of the protein from *Penicillium chrysogenum* as templates. The models were protonated in silico (pH 7.0) by use of *pdbtopqr* and the resulting *pqr* files and the electrostatic potentials of the

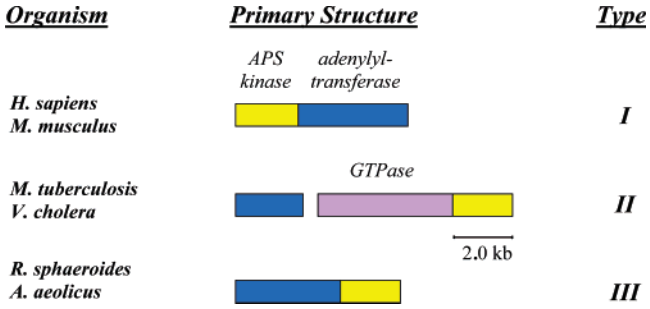

FIGURE 1: Structural gene organization defines the three types of sulfate activating complexes. APS kinase domains (yellow) are quite similar among the three types. The type I and III adenylyltransferase domains (blue) are similar to one another but differ considerably (length and sequence) from that of type II, which is the only SAC that harbors a GTPase (lavender). Joined rectangles indicate domains in a single open reading frame.

surfaces were calculated with the adaptive Poisson−Boltzmann solver algorithm [APBS (*41*−*43*)] at the Gemstone server.

RESULTS AND DISCUSSION

Selecting SAC Candidates. Differences in primary sequence naturally separate the sulfate activating complexes into three basic types; see Figure 1. Types 1 and III are encoded on a single polypeptide that contains two well-conserved catalytic domains: the adenylyltransferase and APS kinase domains. These types are distinguished by a switch in the N- and C-terminal positions of the domains. A less obvious distinction is that the function of the type I APS kinase domain appears, generally, to have been carefully maintained while that of type III varies with species: certain Kinase domains have no known function (*44*), others exhibit partial function (PAPS binding; *40*, *45*), and still others are capable of full catalytic activity. Organisms that express kinase-inactive SACs typically also express an active, single-domain APS kinase. The coding region of the type II adenylyltransferase differs considerably from that of the type I/III domain; moreover, the type II SAC contains a GTPase, a separate polypeptide whose C-terminus encodes the SAC APS kinase domain, which is similar to that of types I and III. To test the hypothesis that substrate channeling is used by these systems to accomplish the catalytic task of activating sulfate, a single representative from each of the SAC types was purified and tested for its ability to channel APS.

Channeling Assay. A direct means of assessing the extent to which a system channels is to determine whether the putative channeled intermediate (APS) enters bulk solvent during steady-state turnover. Comparing the rate at which the intermediate enters solvent to the rate at which total intermediate (channeled and nonchanneled) forms determines how the intermediate partitions and, hence, the channeling efficiency of the system. The experimental challenge, then, is to design measurements that allow accurate comparison of the initial rates of formation of solution-phase and total intermediate.

The initial rate at which total APS forms is determined readily: ADP produced upon phosphorylation of APS is coupled (1:1) to NADH oxidation via pyruvate kinase and lactate dehydrogenase (*28*). To minimize the lag associated with multiple coupling-enzyme assays (*46*) and to prevent

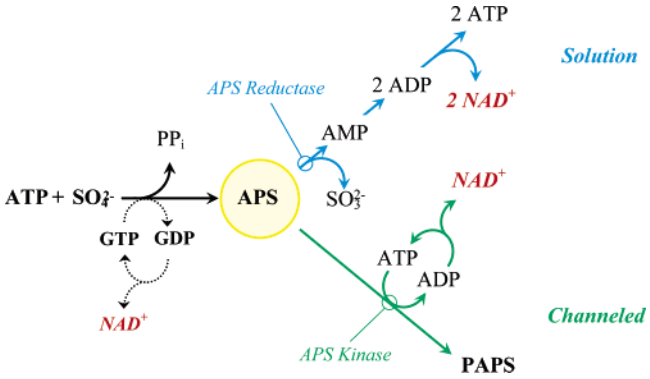

FIGURE 2: Channeling assay scheme. APS formed at the active site of the adenylyltransferase domain (indicated by the yellow dot) has two possible forward reaction fates: either it enters solution (blue path) or it is channeled to the APS kinase domain (green path). If channeled, it is phosphorylated, producing 1 equivalents of ADP, which ultimately leads to the production of 1 equiv of NAD^+ via the PK/LDH coupling system. Only the APS released into solution is reduced to sulfite and AMP, by APS reductase, which is converted to 2 equiv of ADP, by adenylate kinase, and ultimately to 2 equiv of NAD^+.

accumulation of APS to concentrations that could inhibit the APS domain, APS kinase from yeast, which does not contain an adenylyltransferase domain, was added. Determining the initial rate at which solution APS forms can be accomplished by use of a suitably efficient coupling enzyme that acts on APS, which, because it is physically separate from the channeling complex, reports only the APS that is released into solution. Accurate measurement of the rate of APS release requires that the catalytic efficiency ($k_{cat}/K_{m\ APS}$) of the coupling enzyme be sufficiently high, relative to that of the APS kinase domain, that virtually all of the solution-phase APS is "captured" by the coupling enzyme.

APS reductase (EC 1.8.99.2) from *M. tuberculosis* was selected to detect solution-phase APS. The enzyme is a member of an emerging class of reductases that appear, on the basis of their primary sequences, to be progenitors of PAPS reductases (*25*, *30*). The catalytic behavior of the *M. tuberculosis* enzyme has not yet been well characterized. The enzyme catalyzes the two-electron reductive cleavage of APS to produce AMP and SO_3^{2-} (reaction 4):

$$APS^{2-} + 2\ e^- \leftrightarrows APS^{2-} + SO_3^{2-} \qquad (4)$$

AMP can be converted enzymatically to 2 ADP, by adenylate kinase, and then to the oxidation of 2 equiv of NADH, via the PK/LDH system. APS reductase from *M. tuberculosis* was cloned, expressed in *E. coli*, purified, and characterized (see Materials and Methods). The initial-rate constants reveal that while the enzyme is capable of using either APS or PAPS as a substrate [$K_{m\ APS} = 0.57\ (\pm 0.01)\ \mu M$, $k_{cat} = 9.2\ (\pm 0.1)\ min^{-1}$; $K_{m\ PAPS} = 31\ (\pm 3.0)\ \mu M$, $k_{cat} = 0.7\ (\pm 0.3)\ min^{-1}$], APS is reduced far more efficiently than PAPS: $(k_{cat}/K_m)_{APS}/(k_{cat}/K_m)_{PAPS} = 800$.

Once formed at the active site of the adenylyltransferase domain, APS has two possible forward-reaction fates; see Figure 2. It either enters bulk solvent, where it can be acted upon by APS reductase and coupled to the oxidation of 2 equiv of NADH, or it can channel to the APS kinase domain, where it is converted to PAPS and linked to the oxidation of 1 equiv of NADH. The difference in NAD^+/APS

Table 2: Sulfate Activating Complex Initial-Rate Parameters

parameters and reactants	SAC type I	SAC type II[a]	SAC type III
	ATP Sulfurylase		
K_m (μM) for ATP	52 (1)[b]	35 (1)	150 (30)
K_m (μM) for SO_4	490 (50)	390 (5)	1000 (70)
k_{cat} (min^{-1})	1.6 (0.5)	7.8 (0.1)	80 (2)
	APS Kinase		
K_m (μM) for ATP	*c*	77 (3)	24 (0.7)
K_m (μM) for APS	0.012 (0.002)	0.3 (0.01)	0.3 (0.01)
k_{cat} (min^{-1})	0.25 (0.01)	35 (1)	260 (4)

[a] Type II parameters were determined previously (*10*). [b] Numbers in parentheses indicate 1 standard deviation unit. [c] Not determined.

stoichiometry associated with the channeled and nonchanneled paths provides a direct means of determining the channeling efficiency of a given SAC. The equivalent of GDP produced by the type II SAC per APS is also coupled to an equivalent of NAD^+ and must be considered in the stoichiometry analysis.

Establishing conditions for channeling assays required that initial-rate parameters for the forward reactions of the adenylyltransferase and APS kinase domains of type I, II, and III SACs be determined. The reported kinetic parameters for the type I system (*H. sapiens*) differ considerably (*36*, *47*−*49*); hence these parameters were determined under the conditions of the channeling experiment. Type II SAC has been characterized previously by this laboratory (*10*). The type III system has not yet been characterized. The constants are compiled in Table 2, and the assays used to obtain them are described under Materials and Methods (*10*).

To ensure that the catalytic efficiency of APS reductase was high enough relative to that of APS kinase that virtually all of the solution-phase APS was trapped by APS reductase, the ratio of the initial rates of APS synthesis (with/without reductase) was monitored as a function of the concentration of APS reductase at a fixed concentration of APS kinase. As the APS reductase concentration increases relative to that of APS kinase, the fraction of nonchanneled APS converted to AMP, rather than PAPS, increases until the reductase concentration is high enough to capture essentially all of the solution APS, at which point the initial-rate ratio plateaus. It is the relative rate in the plateau that defines the channeling efficiency of the system.

Titrations were performed with representatives from each of the three SAC classes (Figure 3). The type I SAC (*H. sapiens*) titration plateaus at a relative rate of 2.0, the value predicted for a system that does not channel. Thus, within the error of the measurement (~±5%) this system does not channel. This finding contradicts an earlier report (*47*, *50*, *51*) that this system does channel (see below). The type II system (*M. tuberculosis*) yields a plateau at a relative initial rate of 1.5. Type II SACs hydrolyze one GTP per APS formed (*11*, *12*). A type II system that channels produces two NAD^+ per PAPS formed, whereas one that does not channel produces three NAD^+ per APS formed; GDP produces one NAD^+, and APS, which is converted to AMP, produces two (see Figure 2). Nonchanneling type II systems are expected to exhibit a plateau at $^3/_2$, or 1.5, which is precisely what is observed; hence, type II SAC does not channel APS. Unlike type I and II SACs, the initial-rate ratio of the type III system, predicted to plateau at 2 if channeling

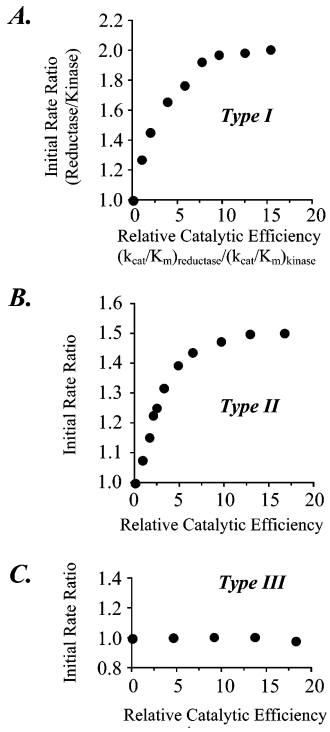

FIGURE 3: Channeling in the type I, II and III sulfate activating complexes. The initial rate of NAD^+ formation is plotted as a function of the ratio of the catalytic efficiencies ($V_m/K_{m\ aps}$) of APS reductase and APS kinase domain, known as the relative catalytic efficiency. The initial rate in the presence of APS reductase was divided by that obtained in its absence to yield the relative initial rate. The assay scheme is outlined in Figure 2. In the absence of APS reductase, yeast APS kinase, which does not contain an adenylyltransferase domain, was added (8.0 units/mL) to prevent a lag in NAD^+ formation and prevent accumulation of inhibitory concentrations of APS. (A) Type I SAC from *H. sapiens*. The reaction mixture contained SAC (0.8 μM), thioredoxin (37 μM), PK (8.0 units/mL), LDH (6.0 units/mL), PP_iase (1.0 units/mL), adenylate kinase (6.0 units/ mL), KCl (50 mM), DTT (2.0 mM), GSH (5.0 mM), PEP (3.0 mM), NADH (0.25 mM), ATP (3.0 mM, $58K_m$), SO_4^{-2} (6.0 mM, $12K_m$), $MgCl_2$ (5.0 mM), Hepes (50 mM, pH 8.0), and APS reductase (1.0, 2.0, 4.0, 6.0, 8.0, 10, 13, or 16 μM), $T = 25 \pm 2$ °C. (B) Type II SAC from *M. tuberculosis*. Except for the following differences, the conditions were identical to those described for panel A. The reaction mixture contained SAC (0.1 μM), GTP (1.0 mM, $83K_m$), ATP (2.0 mM, $57K_m$), SO_4^{-2} (6.0 mM, $15K_m$), and APS reductase (0.60, 1.1, 1.4, 1.7, 2.3, 3.4, 4.6, 6.9, 9.2, or 12.0 μM). (C) Type III SAC from *R. sphaeroides*. Except for the following differences, the conditions were identical to those described for panel A. The reaction mixture contained SAC (19 nM), ATP (2.0 mM, $13K_m$), SO_4^{-2} (6.0 mM, $6.0K_m$), $MgCl_2$ (4.0 mM), Hepes (50 mM, pH 8.0), and different concentrations of APS reductase (4.8, 9.6, 14, or 19 μM).

does not occur, remains fixed at a value of 1 as a function of $(k_{cat}/K_{m\ APS})_{reductase}/(k_{cat}/K_{m\ APS})_{kinase}$. The independence of the initial-rate ratio from the presence of APS reductase demonstrates that *R. sphaeroides* type III SAC efficiently channels APS between its adenylyltransferase and APS kinase sites. It should be noted that similar relative catalytic efficiency ranges were used in each of the titrations; hence the nonchanneling systems provide controls for the type III experiment in that they demonstrate that the relative-efficiency range used in the experiment is capable of essentially quantitative capture of solution APS by the APS reductase in the range corresponding to the plateau.

Independent Confirmation of Substrate Channeling. The channeling titration assays, while conceptually straightfor-

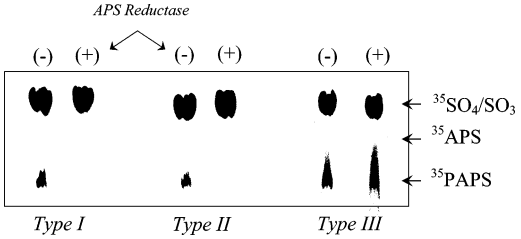

FIGURE 4: Effect of APS reductase on PAPS formation. The incorporation of radiolabel from $[^{35}S]SO_4^{2-}$ into [^{35}S]PAPS was monitored in the presence **(+)** and absence **(−)** of APS reductase. Reaction conditions were identical to those used for the beginning and end points of the corresponding APS reductase titrations (see Figure 3 caption), with the exception that the sulfate concentration (0.20 mM, 150 μCi/mL) was decreased to enhance sensitivity. Reactions were quenched, and radiolabeled reactants were separated by TLC. The APS reductase-induced disappearance of [^{35}S]PAPS from the type I and II reactions indicates that [^{35}S]APS enters bulk solvent where it is converted to AMP and $[^{35}S]SO_3^{2-}$ (which comigrates with $[^{35}S]SO_4^{2-}$). [^{35}S]PAPS synthesis by the type III system is not diminished by addition of APS reductase, supporting the idea that this system channels APS.

ward, are technically involved. For example, the type II titration assay exhibits eight simultaneous catalytic activities during the steady state (see Figure 2). To confirm that NAD^+ formation faithfully reports the partitioning of APS between the bulk solvent and the surface of the protein, the incorporation of radiolabel from $[^{35}S]SO_4^{2-}$ into [^{35}S]PAPS was monitored in the presence and absence of APS reductase under conditions that mimic those used in titrations (see Figure 4). If APS is released into solvent, it will be siphoned away by APS reductase and never "reach" PAPS. If it is channeled, it will remain inaccessible to the reductase, and PAPS formation will not be effected. Thus, PAPS formation is diminished by APS reductase only for those systems that do not channel. Reactions were run under conditions that correspond to the beginning and end points used in the APS reductase titrations [i.e., 0 and maximum values of $(k_{cat}/K_{m\ APS})_{reductase}/(k_{cat}/K_{m\ APS})_{kinase}$]. The reactions were quenched, and radiolabeled reactants were separated by anion-exchange TLC and quantitated (*11*, *52*). The TLC system separates APS and PAPS well but does not separate SO_4^{2-} from SO_3^{2-}. Reactions were run to ≤25% of their end points in all cases. Little if any [^{35}S]APS is detected in the reactions because the catalytic efficiency of APS kinase is far greater than that of the adenylyltransferase. The addition of APS reductase to the SAC I and II reactions causes PAPS formation to decrease to undetectable levels, indicating that these systems release APS into solution. The type III reaction, however, exhibits essentially the same level of PAPS in the presence and absence of APS reductase, supporting the idea that this system channels APS. The ^{35}S labeling and titration assays are in complete agreement: type III SAC channels APS, and types I and II do not.

Previous Reports of Channeling in Type I Systems. Two very similar type I systems (human and mouse brain) have been reported to channel (*47*, *50*, *51*). The predicted primary-sequence lengths of these two systems are identical (624 amino acids), and the sequences differ by conservative substitution at only six positions (less than 1% conservative replacement). The following recent evidence has been used to suggest that the human system might not channel APS: first, the APS concentration increases to levels far greater than that of active sites during steady-state turnover in the forward direction (*36*) (thus, if it occurs, the channeling must be inefficient); second, the structure of the human type 1 SAC shows no evidence of a channel (*53*). The present findings demonstrate that the human type 1 channels either very poorly (≤5% efficiency) or not at all. While these discrepancies might be explained by the seemingly slight differences in buffer conditions used in the different studies, it seems more likely that they are due to experimental pitfalls associated with the isotope-dilution method, which was used to assess channeling in these earlier studies. Isotope trapping studies typically use a nonradioactive form of the putative channeled intermediate to dilute, or "trap", enzymatically synthesized radioactive intermediate that is released into solution during turnover (*54*). If the diluent (APS) is (as was the case in the earlier work) present at subsaturating concentrations with respect to APS kinase, isotopic throughput to PAPS is not affected by the diluent because the velocity of the kinase scales linearly with APS concentration in this regime.

A Plausible Channel. Type III ATP sulfurylases are hexamers—sandwiched, obverted trimers arranged with 3-fold symmetry around a central pore and offset by 60°—giving the hexamer the appearance of a six-pointed star. These structures present an architecture that seems capable of surface transport of the nucleotide. A groove connects each adenylyltransferase active site to the nearest-neighbor APS kinase active site situated in the trimer beneath it. ATP sulfurylase from *P. chrysogenum*, a mold, harbors an APS kinase domain that, while incapable of catalysis, is able to bind PAPS, resulting in an allosteric downregulation of the adenylyltransferase activity (*45*, *55*). Structures of the *P. chrysogenum* enzyme in which the binding pocket of the APS kinase domain is either occupied, by APS, or empty are believed to represent the allosterically altered and unaltered structures, respectively. The similar length (99.3%) and sequence (54% identity, 29% similarity) of the *P. chrysogenum* and *R. sphaeroides* SAC primary sequences suggested that the *P. chrysogenum* crystal structures (*39*, *40*) would provide excellent templates for developing models of the *R. sphaeroides* SAC.

Models of the R- and T-state structures were constructed, and the electrostatic potential at the van der Waals surfaces of these structures are presented in Figure 5. Nucleotide (APS or PAPS) positioned at the adenylyltransferase active site is shown in green, while that at the APS kinase binding pocket is shown in yellow. (APS at the adenylytransferase site was added as a visual cue; it is not present the in the T-state template, while the R-state template has APS positioned at both sites.) The distance between the two binding sites, measured along the channel, is ∼75 Å. The channel undergoes a remarkable change in shape and chemical disposition as the system moves from the R- to the T-state. The long edges on either side of the channel move toward one another in the R configuration, as if to seal the convoluted cylindrical space linking the two binding sites, perhaps to regulate solvent access during the early stages of transfer. At the point of closest approach, the C_α edges of the cylinder are ∼10 Å apart. This minimum distance increases to ∼25 Å in the T-state, resulting in a significant opening of the channel, perhaps to release product at the end of the catalytic cycle. The models, which are presumed

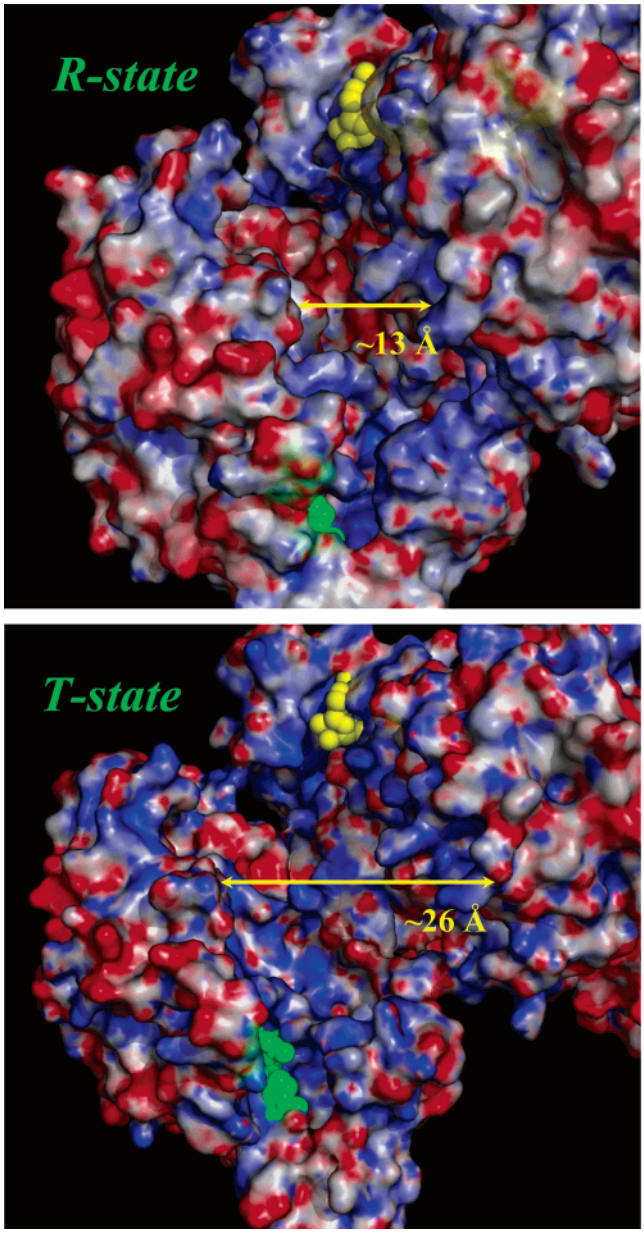

FIGURE 5: Electrostatic potential surfaces of R- and T-state models of the type III SAC from *R. sphaeroides*. Models were constructed with Swiss-Model (*37*, *38*), with *P. chrysogenum* templates (*39*, *40*) protonated in silico (pH 7.0), and the electrostatic potential surface was calculated by use of the adaptive Poisson−Boltzmann solver (APBS) algorithm (*41*−*43*) and rendered by use of *Pymol*. Nucleotide at the adenylyltransferase and APS kinase sites are shown in green and yellow, respectively. APS positioned at the adenylyltransferase site in the T-state structure serves solely as a visual cue; it is not present in the template structure. The groove connecting the active sites measures ~75 Å in length and opens considerably upon binding of PAPS at the APS kinase active site (see T-state structure).

to be catalytic intermediates, predict that the electrostatics of the channel's inner lining change radically during the R- to T-state transformation. "Pools" of positive charge (~ 70 Å^2) migrate away from central aspects of the channel and are replaced by comparably sized pools of negatively charge that emerge during the transition. One cannot help but wonder how, and to what extent, such spatiotemporal changes in chemical potential might be linked to motion of the nucleotide. These issues are currently under close scrutiny in this laboratory.

CONCLUSIONS

Representatives from each of the three types of sulfate activating complex were tested for the ability to channel APS between their adenylyltransferase and APS kinase active sites. By use of an assay that detects optically the deposition of APS into bulk solvent during steady-state turnover, it was shown that neither type I nor type II systems channel with appreciable efficiency (≤5%); however, the channeling efficiency of the type III complex is quite high, ≥95%. Structural models of the type III complex reveal a 75 Å-long groove that interconnects the active sites and that appears to open and close in response to the position of the channeled nucleotide. The changes in the electrostatic potential of the groove that occur as it opens and closes are considerable and may be coupled to movement of the nucleotide.

REFERENCES

1. Rhee, S., Parris, K. D., Ahmed, S. A., Miles, E. W., and Davies, D. R. (1996) Exchange of K^+ or Cs^+ for Na^+ induces local and long-range changes in the three-dimensional structure of the tryptophan synthase α2β2 complex, *Biochemistry 35*, 4211−21.
2. Thoden, J. B., Holden, H. M., Wesenberg, G., Raushel, F. M., and Rayment, I. (1997) Structure of carbamoyl phosphate synthetase: a journey of 96 Å from substrate to product, *Biochemistry 36*, 6305−16.
3. Knighton, D. R., Kan, C. C., Howland, E., Janson, C. A., Hostomska, Z., Welsh, K. M., and Matthews, D. A. (1994) Structure of and kinetic channelling in bifunctional dihydrofolate reductase−thymidylate synthase, *Nat. Struct. Biol. 1*, 186−94.
4. Perham, R. N. (2000) Swinging arms and swinging domains in multifunctional enzymes: catalytic machines for multistep reactions, *Annu. Rev. Biochem. 69*, 961−1004.
5. Meier, I. (2005) Nucleocytoplasmic trafficking in plant cells, *Int. Rev. Cytol. 244*, 95−135.
6. Hosse, R. J., Rothe, A., and Power, B. E. (2006) A new generation of protein display scaffolds for molecular recognition, *Protein Sci. 15*, 14−27.
7. Marx, A., Muller, J., and Mandelkow, E. (2005) The structure of microtubule motor proteins, *Adv. Protein Chem. 71*, 299−344.
8. Leyh, T. S. (1993) The physical biochemistry and molecular genetics of sulfate activation, *Crit. Rev. Biochem. Mol. Biol. 28*, 515−42.
9. Robbins, P. W., and Lipmann, F. (1958) Enzymatic synthesis of adenosine-5′-phosphosulfate, *J Biol. Chem. 233*, 686−90.
10. Sun, M., Andreassi, J. L., 2nd, Liu, S., Pinto, R., Triccas, J. A., and Leyh, T. S. (2005) The trifunctional sulfate-activating complex (SAC) of *Mycobacterium tuberculosis*, *J. Biol. Chem. 280*, 7861−6.
11. Liu, C., Suo, Y., and Leyh, T. S. (1984) The energetic linkage of GTP hydrolysis and the synthesis of activated sulfate, *Biochemistry 33*, 7309−14.
12. Sun, M., and Leyh, T. S. (2005) Anatomy of an energy-coupling mechanism−the interlocking catalytic cycles of the ATP sulfurylase−GTPase system, *Biochemistry 44*, 13941−8.
13. Haldane, J. B. S. (1965) *Enzymes*, MIT Press, Cambridge, MA.
14. Albery, W. J., and Knowles, J. R. (1976) Evolution of enzyme function and the development of catalytic efficiency, *Biochemistry 15*, 5631−40.
15. Satishchandran, C., and Markham, G. D. (1989) Adenosine-5′-phosphosulfate kinase from *Escherichia coli* K12. Purification, characterization, and identification of a phosphorylated enzyme intermediate, *J. Biol. Chem. 264*, 15012−21.
16. MacRae, I. J., and Segel, I. H. (1999) Adenosine 5′-phosphosulfate (APS) kinase: diagnosing the mechanism of substrate inhibition, *Arch. Biochem. Biophys. 361*, 277−82.
17. Lillig, C. H., Schiffmann, S., Berndt, C., Berken, A., Tischka, R., and Schwenn, J. D. (2001) Molecular and catalytic properties of *Arabidopsis thaliana* adenylyl sulfate (APS)-kinase, *Arch. Biochem. Biophys. 392*, 303−10.
18. Wei, J., Tang, Q. X., Varlamova, O., Roche, C., Lee, R., and Leyh, T. S. (2002) Cysteine biosynthetic enzymes are the pieces of a metabolic energy pump, *Biochemistry 41*, 8493−8.

19. Leyh, T. S., Taylor, J. C., and Markham, G. D. (1988) The sulfate activation locus of *Escherichia coli* K12: cloning, genetic, and enzymatic characterization, *J. Biol. Chem. 263*, 2409−16.
20. Wei, J., and Leyh, T. S. (1998) Conformational change rate-limits GTP hydrolysis: the mechanism of the ATP sulfurylase−GTPase, *Biochemistry 37*, 17163−9.
21. Zhang, H., Varlamova, O., Vargas, F. M., Falany, C. N., and Leyh, T. S. (1998) Sulfuryl transfer: the catalytic mechanism of human estrogen sulfotransferase, *J. Biol. Chem. 273*, 10888−92.
22. Spiegelberg, B. D., Xiong, J. P., Smith, J. J., Gu, R. F., and York, J. D. (1999) Cloning and characterization of a mammalian lithium-sensitive bisphosphate 3′-nucleotidase inhibited by inositol 1,4-bisphosphate, *J. Biol. Chem. 274*, 13619−28.
23. Andreassi, J. L., 2nd, and Leyh, T. S. (2004) Molecular functions of conserved aspects of the GHMP kinase family, *Biochemistry 43*, 14594−601.
24. Pilloff, D., Dabovic, K., Romanowski, M. J., Bonanno, J. B., Doherty, M., Burley, S. K., and Leyh, T. S. (2003) The kinetic mechanism of phosphomevalonate kinase, *J. Biol. Chem. 278*, 4510−5.
25. Bick, J. A., Dennis, J. J., Zylstra, G. J., Nowack, J., and Leustek, T. (2000) Identification of a new class of 5′-adenylylsulfate (APS) reductases from sulfate-assimilating bacteria, *J. Bacteriol. 182*, 135−42.
26. Noda, L., and Kuby, S. A. (1936) Myokinase, ATP−AMP transphosphorylase: 2 ADP = ATP + AMP, *Methods Enzymol. 6*, 223−230.
27. Noda, L. (1973) in *The Enzymes* (Boyer, P. D., Ed.) pp 279−305, Academic Press, New York.
28. Bucher, T., and Pfleiderer, G. (1995) Pyruvate kinase from muscle: pyruvate phosphokinase, pyruvic phosphotransferase, phosphopyruvate transphosphorylase, phosphate-transferring enzyme II, ect. phosphoenolypyruvate + ADP = pyruvate + ATP, *Methods Enzymol. 1*, 435−440.
29. Carroll, K. S., Gao, H., Chen, H., Leary, J. A., and Bertozzi, C. R. (2005) Investigation of the iron-sulfur cluster in *Mycobacterium tuberculosis* APS reductase: implications for substrate binding and catalysis, *Biochemistry 44*, 14647−57.
30. Carroll, K. S., Gao, H., Chen, H., Stout, C. D., Leary, J. A., and Bertozzi, C. R. (2005) A conserved mechanism for sulfonucleotide reaction, *PLoS Biol. 3*, 1418−1435.
31. Burkart, M. D., and Wong, C. H. (1999) A continuous assay for the spectrophotometric analysis of sulfotransferases using aryl sulfotransferase IV, *Anal. Biochem. 274*, 131−7.
32. Takehara, K., Kubushiro, K., Iwamori, Y., Tsukazaki, K., Nozawa, S., and Iwamori, M. (2001) Expression of an isoform of the testis-specific estrogen sulfotransferase in the murine placenta during the late gestational period, *Arch. Biochem. Biophys. 394*, 201−8.
33. Leyh, T. S., and Suo, Y. (1992) GTPase-mediated activation of ATP sulfurylase, *J Biol. Chem. 267*, 542−5.
34. Lyle, S., Geller, D. H., Ng, K., Stanczak, J., Westley, J., and Schwartz, N. B. (1994) Kinetic mechanism of adenosine 5′-phosphosulphate kinase from rat chondrosarcoma, *Biochem. J. 301* (Pt 2), 355−9.
35. Venkatachalam, K. V., Akita, H., and Strott, C. A. (1998) Molecular cloning, expression, and characterization of human bifunctional 3′-phosphoadenosine 5′-phosphosulfate synthase and its functional domains, *J. Biol. Chem. 273*, 19311−20.
36. Lansdon, E. B., Fisher, A. J., and Segel, I. H. (2004) Human 3′-phosphoadenosine 5′-phosphosulfate synthetase (isoform 1, brain): kinetic properties of the adenosine triphosphate sulfurylase and adenosine 5′-phosphosulfate kinase domains, *Biochemistry 43*, 4356−65.
37. Peitsch, M. C. Protein modeling by E-mail, *Bio/Technology 13*, 658−660.
38. Schwede, T., Kopp, J., Guex, N., and Peitsch, M. C. (2003) SWISS-MODEL: An automated protein homology-modeling server, *Nucleic Acids Res. 31*, 3381−5.
39. MacRae, I. J., Segel, I. H., and Fisher, A. J. (2001) Crystal structure of ATP sulfurylase from *Penicillium chrysogenum*: insights into the allosteric regulation of sulfate assimilation, *Biochemistry 40*, 6795−804.
40. MacRae, I. J., Segel, I. H., and Fisher, A. J. (2002) Allosteric inhibition via R-state destabilization in ATP sulfurylase from *Penicillium chrysogenum*, *Nat. Struct. Biol. 9*, 945−9.
41. Holst, M., and Saied, F. (1993) Multigrid solution of the Poisson−Boltzmann equation, *J. Comput. Chem. 14*, 105−113.
42. Holst, M., and Saied, F. (1995) Numerical solution of the nonlinear Poisson−Boltzmann equation: Developing more robust and efficient methods, *J. Comput. Chem. 16*, 337−364.
43. Baker, N. A., Sept, D., Joseph, S., Holst, M. J., and McCammon, J. A. (2001) Electrostatics of nanosystems: application to microtubules and the ribosome, *Proc. Natl. Acad. Sci. U.S.A. 98*, 10037−41.
44. Lalor, D. J., Schnyder, T., Saridakis, V., Pilloff, D. E., Dong, A., Tang, H., Leyh, T. S., and Pai, E. F. (2003) Structural and functional analysis of a truncated form of *Saccharomyces cerevisiae* ATP sulfurylase: C-terminal domain essential for oligomer formation but not for activity, *Protein Eng. 16*, 1071−9.
45. Foster, B. A., Thomas, S. M., Mahr, J. A., Renosto, F., Patel, H. C., and Segel, I. H. (1994) Cloning and sequencing of ATP sulfurylase from *Penicillium chrysogenum*. Identification of a likely allosteric domain, *J. Biol. Chem. 269*, 19777−86.
46. McClure, W. R. (1969) A kinetic analysis of coupled enzyme assays, *Biochemistry 8*, 2782−6.
47. Fuda, H., Shimizu, C., Lee, Y. C., Akita, H., and Strott, C. A. (2002) Characterization and expression of human bifunctional 3′-phosphoadenosine 5′-phosphosulphate synthase isoforms, *Biochem. J. 365*, 497−504.
48. Harjes, S., Scheidig, A., and Bayer, P. (2004) Expression, purification and crystallization of human 3′-phosphoadenosine−5-phosphosulfate synthetase 1, *Acta Crystallogr., Part D 60*, 350−2.
49. Lyle, S., Geller, D. H., Ng, K., Westley, J., and Schwartz, N. B. (1994) Kinetic mechanism of ATP-sulphurylase from rat chondrosarcoma, *Biochem. J. 301* (Pt 2), 349−54.
50. Lyle, S., Ozeran, J. D., Stanczak, J., Westley, J., and Schwartz, N. B. (1994) Intermediate channeling between ATP sulfurylase and adenosine 5′-phosphosulfate kinase from rat chondrosarcoma, *Biochemistry 33*, 6822−7.
51. Lyle, S., Stanczak, J. D., Westley, J., and Schwartz, N. B. (1995) Sulfate-activating enzymes in normal and brachymorphic mice: evidence for a channeling defect, *Biochemistry 34*, 940−5.
52. Liu, C., Wang, R., Varlamova, O., and Leyh, T. S. (1998) Regulating energy transfer in the ATP sulfurylase−GTPase system, *Biochemistry 37*, 3886−2.
53. Harjes, S., Bayer, P., and Scheidig, A. J. (2005) The crystal structure of human PAPS synthetase 1 reveals asymmetry in substrate binding, *J. Mol. Biol. 347*, 623−35.
54. Spivey, H. O., and Ovadi, J. (1999) Substrate channeling, *Methods 19*, 306−21.
55. MacRae, I., and Segel, I. H. (1997) ATP sulfurylase from filamentous fungi: which sulfonucleotide is the true allosteric effector? *Arch. Biochem. Biophys. 337*, 17−26.

BI060421E